Imaging the Effect of Dielectric Breakdown in a Multilayered Polymer Film

Mason A. Wolak,[1] Alan S. Wan,[2] James S. Shirk,[1] Matt Mackey,[3] Anne Hiltner,[3] Eric Baer[3]

[1]*Optical Sciences Division, U.S. Naval Research Laboratory, Washington, DC 20375*
[2]*Evans Analytical Group, East Windsor, NJ 08520*
[3]*Department of Macromolecular Science and Center for Applied Polymer Research, Case Western Reserve University, Cleveland, OH 44106-7202*

Received 17 September 2010; accepted 8 January 2011
DOI 10.1002/app.34269
Published online 31 August 2011 in Wiley Online Library (wileyonlinelibrary.com).

ABSTRACT: The dielectric strength and energy storage capability of poly(vinylidene fluoride-hexafluoropropylene) copolymer (P[VDF-HFP]) films are enhanced by interleaving layers of PVDF copolymer with thin layers of polycarbonate (PC). To gain insight into the breakdown processes in such materials, focused ion beam (FIB) milling in conjunction with scanning electron microscopy (SEM) was used to study the effect of a breakdown on the film. FIB can sequentially mill cross sections that are each imaged by SEM. The technique can provide quasi-3D images across the film and give a detailed view of the damage caused by an electrical breakdown. Here, breakdowns initiated using a needle-plane electrode configuration were imaged. In homogeneous films, the damage was confined to the small volume at the pinhole site. In 32-layer 50/50 PC/P[VDF-HFP] multilayer films, damage extending laterally up to $\sim$ 15 μm into the film along the layer interfaces was seen. In addition to the delamination, layer buckling and distortion were apparent. The damage varied with the sample orientation, but the images indicate that the interfaces play an important role in the breakdown. They suggest that modifying the interface properties can be a strategy to further improve the dielectric strength of multilayer polymer dielectric materials. © 2011 Wiley Periodicals, Inc[†]. J Appl Polym Sci 123: 2548–2557, 2012

Key words: focused ion beam (FIB); scanning electron microscopy (SEM); multilayer composite; dielectric properties; polycarbonates; poly(vinylidene fluorides)

INTRODUCTION

The development of high energy density dielectric materials is critical to the advancement of smaller, lighter, and more economical electrical devices and power systems. Polymer films are widely used as the active dielectric medium in high energy density capacitors, because they exhibit high dielectric strength, low dielectric loss, high energy density, fast speed, and high reliability.[1]

We have reported that multilayered polymer films containing many thin alternating layers of polycarbonate (PC) and a poly(vinylidene fluoride-hexafluoropropylene) copolymer (P[VDF-HFP]) exhibit a higher dielectric strength (E_B) than films of either polymer alone.[2,3] For example, films comprising 50 vol % PC/50 vol % P[VDF-HFP] display $E_B > 750$ kV/mm and a permittivity (ε_r) of 5.4 at 100 Hz. For a capacitor based on a linear dielectric material, the maximum stored energy density (U_d) is proportional to the effective permittivity (ε_r) times the square of the dielectric strength (E_B). The increase in dielectric strength provides a corresponding increase in deliverable energy density. An energy density, U_d, of $\sim$ 13.5 J/cm^3 was reported for small parallel plate capacitors based on a 256-layer 50 vol % PC/50 vol % P[VDF-HFP] composite. This layered structure provided a 60% increase in energy density compared with capacitors based on P[VDF-HFP] alone.

The permittivity of such a multilayer polymer is reasonably described by an effective medium model, but the reason for the increased dielectric strength is not yet fully understood. In a previous article, it was suggested that the increase in dielectric strength of the nanolayered materials resulted from a "barrier" effect.[4–8] This is a well-known effect in composites where material boundaries present barriers to the propagation of a dielectric breakdown across the film. In further studies of a breakdown induced by an inhomogeneous field, it was found that the details of the breakdown and the charge dissipated therein depend on factors including the orientation of the layers, the thickness of the film, and the polarity of the electrodes.[3] It was also shown that the breakdown processes in layered films included the formation of damage structures with a "tree-like" appearance.

Correspondence to: M. A. Wolak (mason.wolak@nrl.navy.mil).

Journal of Applied Polymer Science, Vol. 123, 2548–2557 (2012)

To explore these breakdown processes in polymer films, an analytical technique that has proven to be useful for analyzing damaged regions of failed semiconductor devices[9] was adapted to study the effects of a dielectric breakdown in polymer films. The technique, a combination of focused ion beam (FIB) milling and scanning electron microscopy (SEM), provides images of the spatial variation of the changes resulting from the breakdown.

FIB milling can remove micrometer and submicrometer (<300 nm) thicknesses of a material with high precision. FIB techniques have been used for microfabrication in the integrated circuit industry.[10] When used as part of an analytical technique to examine damage to failed circuits, FIB is used to serially section the material and microscopy, SEM, in this case, provides images of the milled cross sections. The images can be examined sequentially or be combined to form a three-dimensional map of the electrically induced damage.

Although FIB milling of polymer materials is less common, it has been used to mill polymer films. The fabrication of polymer gratings[11] and polymer photonic crystal masters by FIB techniques has been reported.[12,13] There are also reports of using these techniques to image polymer/metal composites.[14,15] This led us to investigate adapting FIB/SEM analysis techniques to examine the effect of a dielectric breakdown in failed polymer film dielectric materials. The FIB/SEM technique makes it possible to examine the changes in the layer structure as a function of distance from a breakdown site. Changes in the layer structure caused by the dielectric breakdown are found by comparing images of cross sections of "as fabricated" films with those after a breakdown. Sequential images through the multilayered film show how voids and channels created by localized discharges or by the breakdown develop and evolve as a function of distance from the primary break down site, which is typically a 30–70 μm pinhole.

We demonstrate the technique and then use it to compare the effect of a breakdown in homogeneous films of PC and P[VDF-HFP] and layered films where thin layers of PC are alternated with thin P[VDF-HFP] layers. The layered films had 32 layers with approximately equal PC and P[VDF-HFP] layer thicknesses. Thirty-two-layer films were chosen for these studies to ensure that the individual layers were thick enough (>350 nm) to be easily resolved via SEM. The 50/50 composition films were chosen because they exhibit a substantial increase in the dielectric strength relative to homogeneous control films.

EXPERIMENTAL

Film fabrication

Thirty-two-layer films containing alternating layers with equivalent volumes of PC and P[VDF-HFP] were prepared using the melt coextrusion method previously reported.[16,17] Makrolon 2207 was used for the PC component and Solef 21508 [—$(CH_2—CF_2)_{85}$—$(CFCF_3CF_2)_{15}$—] for the P[VDF-HFP] component. Single component (homogeneous) films were also prepared by the same melt coextrusion method. The films were produced with polyethylene skin layers to protect the film surfaces. The polyethylene layers were removed prior to imaging or the application of high field.

Preparation of dielectric breakdown samples

A set of 32-layer 50/50 PC/P[VDF-HFP] films was divided into two groups: one was preserved as control films and the other was subjected to a divergent electric field using a needle-plane electrode configuration sufficient to cause dielectric breakdown. The films were placed on a brass ground plane electrode and submersed in a high-breakdown fluid (Fluorinert FC-40) to prevent arcing and surface discharge. For a majority of the samples described here, a positive voltage was applied with a tungsten tip (radius $\sim$ 20 μm) placed in direct contact with the top P[VDF-HFP] surface, whereas the bottom PC surface made contact to the ground plane. The reverse configuration, in which the surfaces were flipped with respect to the tip and plane, was also examined. A Quadtech Guardian 12 kV Hi Pot Tester was used as the high-voltage source. Dielectric breakdown was achieved in multilayered films by application of a 12-kV square wave pulse (duration = 200 ms) on samples with thicknesses of 13 μm or less. The same experiment was repeated with homogeneous films of PC and P[VDF-HFP]. For the homogeneous films, the breakdown occurred at applied voltages of less than 10 kV.

Cross section preparation and imaging

Prior to imaging, each sample was sputter coated with a thin layer (5 nm) of Au using a Bal-Tec SD-005 sputter coater. Sequential cross sections of the films were prepared using an FEI brand FIB biased at 30 kV with a Ga^+ current of 7 nA. For large area excavation and cross sections, a selective carbon etch (SCE) technique was employed to expedite the milling process.[15] Any Ga ion implantation in the film should not affect the images of interest here.

To spatially resolve the changes in the polymer structure as a function of distance from the breakdown site, an initial trench was milled completely through the thickness of the film at a distance of about 50–60 μm from the site of breakdown. This trench was about 25–35 μm wide. After imaging the face of this trench, it was extended in a stepwise manner toward the breakdown pinhole by

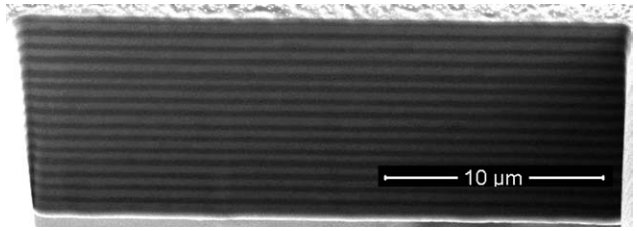

Figure 1 SEM micrograph of a cross section of a typical 32-layer 50 vol % PC/50 vol % P[VDF-HFP] film. The darker layers are PC and the lighter layers are P[VDF-HFP].

successive ion milling. Each cut removed a precisely measured slice of the film. The slices ranged from 500 to 2000 nm thick, with thinner slices milled in areas where notable changes in the layer structure occurred. The imaging trench was extended until it met the breakdown pinhole. Each successive exposed cross section was imaged with an FEI SEM at an angle of 52°, biased at 5 kV with an e-beam current of 0.4 nA. High-magnification images (>3500×) were obtained using an in-lens detector. The "as fabricated" control films were imaged in a similar manner. Sample and layer thicknesses were determined from the recorded images based on the magnification scale parameters adjusted for the imaging angle described above.

RESULTS AND DISCUSSION

FIB/SEM imaging of control films

First, the FIB/SEM technique is used to image the structure of multilayer PC/P[VDF-HFP] films as they are fabricated. These images verify that the FIB/SEM technique has sufficient contrast and resolution to resolve the layer structure. It also permits the examination of any defects in the original films before they have been subjected to an electric field.

Figure 1 displays an SEM image of a 32-layer film with equal volume fractions of PC and P[VDF-HFP]. The cross section displayed in this image was obtained by FIB milling a 35 μm wide trench through the film, followed by imaging the exposed face of the trench. The darker layers are PC, and the lighter layers are P[VDF-HFP]. The layer identities were previously confirmed by comparing images of films with known different volume concentrations and hence different relative layer thicknesses.[2] The contrast can be correlated with the relative electron density in the different polymers.[18,19]

The sample shown in Figure 1 has an overall thickness of 11.7 μm, which corresponds to an expected layer thickness of ~ 365 nm for the individual PC and P[VDF-HFP] layers. The average layer thickness deduced from the SEM image is 356 nm for PC and 375 nm for P[VDF-HFP]. This corresponds to a PC/PVDF volume ratio of 49/51, which is within 1% of the fabrication goal. The standard deviation in the layer thickness in the films used in these experiments was typically between 10% and 15%; in Figure 1 it is about 12%. Figure 2 shows resolved images of 13 μm thick, 128- and 256-layer films. The contrast for this pair of polymers is sufficient to resolve individual layers that are on the order of ~ 50 nm in thickness.

The observed contrast between the PC and P[VDF-HFP] layers is obviously important to the usefulness of the FIB/SEM technique for polymer materials. Polymer materials do not always yield such good contrast in SEM images. Contributions to the strong contrast here probably include the relatively higher electron density of P[VDF-HFP] compared with PC because of the highly electronegative fluorine atoms in P[VDF-HFP]. Charging effects can also play a role in determining the contrast between insulating materials. Because the dielectric constant of P[VDF-HFP] is approximately 3–4 times greater than that of PC, a higher charge accumulation would be expected in the P[VDF-HFP] regions, which could also contribute to the observed brightness and overall contrast between the layers.[20] Although it is probably not important here, resolution of multilayer

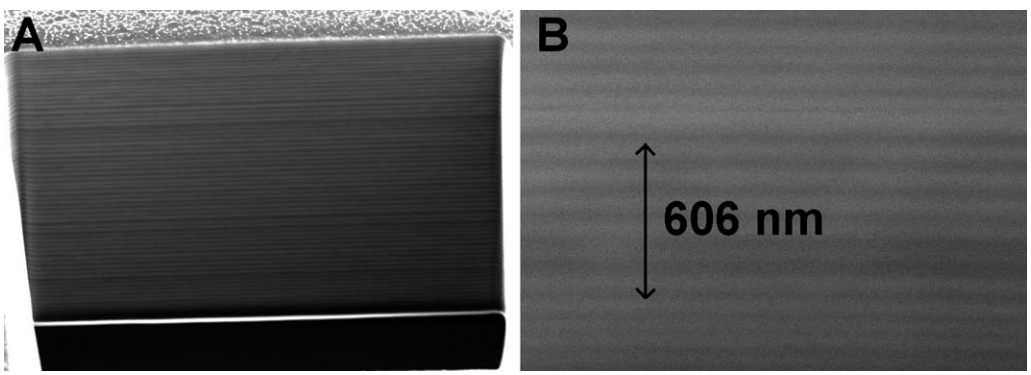

Figure 2 (A) SEM micrograph of a cross section of a 128-layer 50 vol % PC/50 vol % P[VDF-HFP] film. (B) 100,000× SEM micrograph of the layer structure of a 256-layer 50 vol % PC/50 vol % P[VDF-HFP] film with scale bar spanning 12 layers at 606 nm total thickness for an average layer thickness of approximately 50 nm.

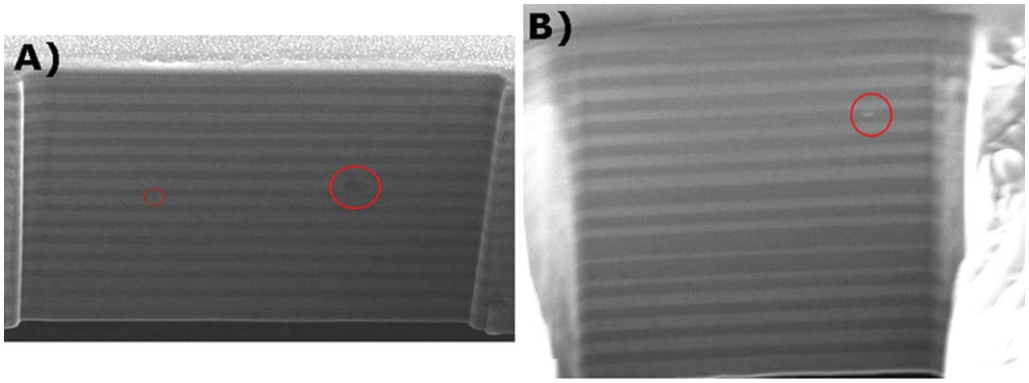

Figure 3 (A) Inhomogeneities or defects in the P[VDF-HFP] layer in a 32-layer 50% PC/50% P[VDF-HFP] control film. These were found in ~ 10% of the images. The approximate size of the larger defect is ~ 300 nm high × 1200 nm wide. (B) Defect in the PC layer found in ~ 3% of the images. The size is ~ 120 nm high × 180 nm wide. [Color figure can be viewed in the online issue, which is available at wileyonlinelibrary.com.]

polymer structures has also been reported using topographical contrast.[21,22] More detailed quantitative estimates of the expected contrast between different polymers have been described elsewhere.[23]

The FIB/SEM imaging technique was found to be useful in evaluating the defects present in multilayer films before they are subjected to an electric field. Except for the variation in layer thickness noted above, any imperfections were rare. To find and characterize defects, several hundred images of different sections of the control films were recorded. Figures 1 and 2 are representative of these images. Continuous discrete layers were observed in all images obtained from control films. There are no obvious defects or delaminations at the interfaces. An example of the most common defect is shown in Figure 3A, where dark ovals are seen within the confines of brighter P[VDF-HFP] layers. These were found in about 10% of images. The darker regions are probably low-density regions, perhaps representing the tail of the molecular weight distribution of the polymer. The volume fraction of these defects was ~ 0.01%. A second type of defect was a smaller bright area within a PC layer. An example is shown in Figure 3B. These were found in ~ 3% of images and represent a volume fraction on the order of a few ppm. At this low level, these may be an impurity or contaminant. No discontinuities, cavities, or voids within the layers or at layer interfaces were observed in any images of the control films prior to the application of high fields.

Breakdown-induced changes—Homogeneous films

After the multilayered control films were imaged, the FIB/SEM technique was used to image the effects of a dielectric breakdown on homogeneous polymer films. A dielectric breakdown involves an electrical discharge across the film. It results in a pinhole through the film at the site of the discharge, typically ranging from 30 to 70 μm in diameter. Sequences of SEM images near the pinhole provide a visualization of the changes in the polymer structure caused by the breakdown. FIB/SEM images were recorded as a function of the distance from the breakdown pinhole.

Figure 4A shows an SEM image of the pinhole in a homogeneous P[VDF-HFP] film caused by a dielectric breakdown. The walls of the breakdown pinhole are relatively smooth except for some flakes of polymer on the sides. This polymer is homogeneous, so no layer structure is observed. The sides of the pinhole walls were milled using FIB to prepare cross sections of the film at various places around the pinhole and SEM images were obtained after each milling cycle. A typical image at 8 μm from the pinhole is shown in Figure 4B. The polymer here is uniform; there is no evidence of any damage due to the dielectric breakdown. A series of several sequential SEM images of cross sections starting at 1 μm out to 50 μm from the pinhole also showed no evidence for electric field-induced changes. We conclude that the breakdown-induced damage to this film is confined to the breakdown pinhole. No voids, cracks, or fissures are observed in the volume surrounding it.

An analogous set of images of the breakdown pinhole and its surroundings in a homogeneous PC film were also acquired. The images were similar to those for the P[VDF-HFP] film. A pinhole was the only visible change. The walls of the pinhole were relatively featureless, and there was no evidence for changes in the polymer beyond the pinhole wall.

These images are consistent with the classical model of dielectric breakdown in a polymer film.[24] In this model, an initial discharge within the film gives rise to a breakdown tree that propagates more or less vertically through the film. Once a

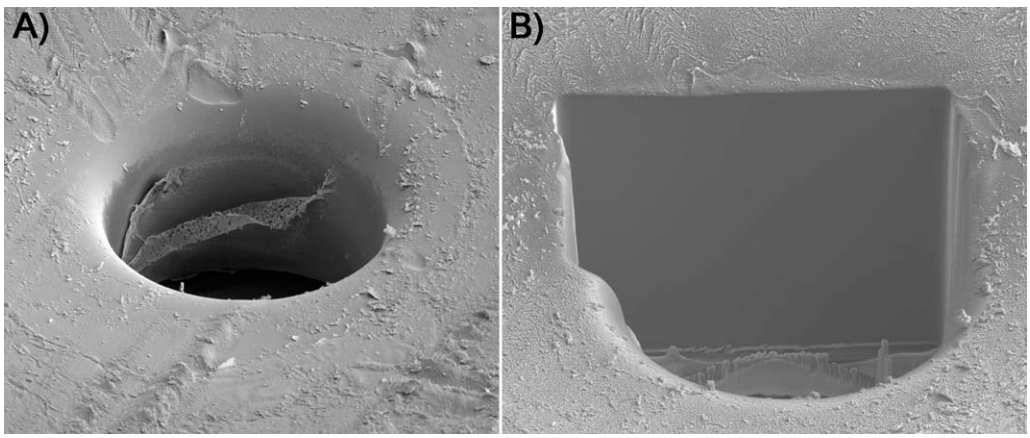

Figure 4 (A) SEM micrograph of a breakdown pinhole ($d = 38$ μm) in a P[VDF-HFP] control film. (B) SEM micrograph of an FIB-prepared cross section of the same film at a distance of ~ 8 μm into the film relative to the pinhole sidewall.

continuous path is reached between the top and bottom electrodes, an electrical discharge passes through the film, vaporizing the polymer and creating a pinhole along the tree path. In the homogeneous polymer films, the breakdown apparently follows a relatively straight path across the film, parallel to the applied field. There is no evidence that it extended beyond the pinhole region.

Breakdown-induced changes—Layered films

In Reference 3, it was shown that the nature of the damage due to an inhomogeneous field breakdown depends on several factors including the orientation of the layers, the polarity of the electrodes, and the film thickness. The most notable tree-like damage was found in the cases where the needle was positive, and the background plane was negative. The present article will discuss data taken with this configuration. The observed damage was also found to depend on the polymer layer that is topmost, nearest the tip.[3] This article concentrates on the effect of a breakdown on a 32-layer 50 vol % PC/50 vol % P[VDF-HFP] film where a P[VDF-HFP] layer is the surface nearest the tungsten tip.

Figure 5A shows the breakdown pinhole in this case. Significant changes in the internal layer structure are apparent. The walls of the breakdown pinhole in the layered film (Fig. 5A) are not nearly as smooth as the walls of the breakdown pinholes in homogeneous films. Features, such as voids and delaminated polymer fragments, can be seen extending into the wall. FIB milling was used to produce sequential cross sections of the film adjacent to the pinhole. An image of one of these in Figure 5B shows that the delaminations extend into the film beyond the pinhole. The layer structure is still visible, although it is distorted to accommodate the voids between the delaminated layers. There is a thin layer of material at the bottom of the pinhole that appears to be polymer that has melted and resolidified.

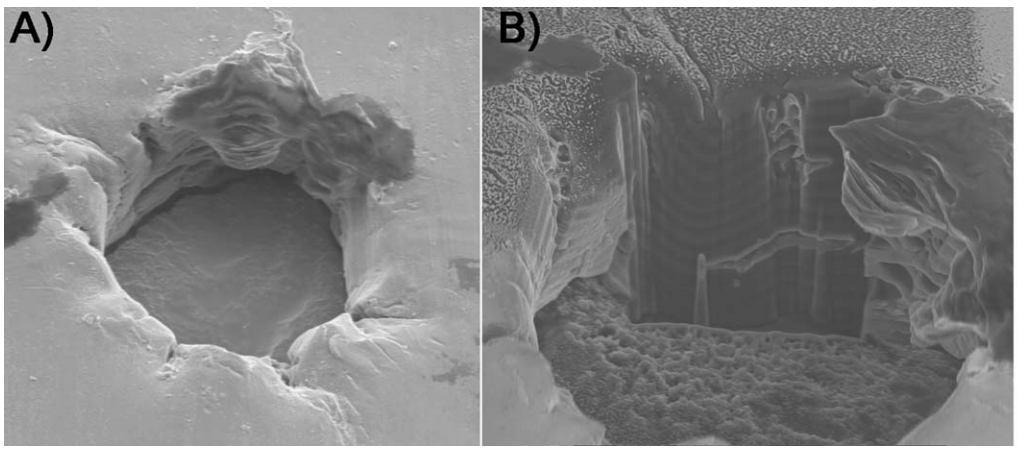

Figure 5 (A) SEM micrograph of a breakdown pinhole ($d = 40$ μm) in a 32-layer 50% PC/50% P[VDF-HFP] film. (B) Cross section of the film at ~ 2 μm into the film relative to the pinhole sidewall. This image was obtained after a 90° clockwise rotation from the orientation shown in (A).

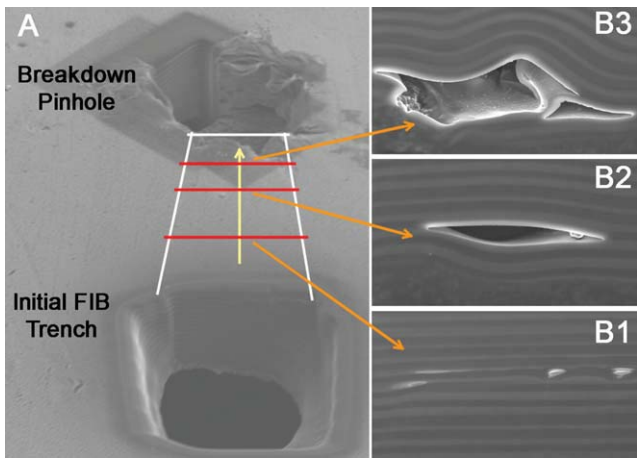

Figure 6 SEM micrograph showing (A) the breakdown pinhole and the initial FIB milled trench in a 32-layer 50 vol % PC/50 vol % P[VDF-HFP] film after a dielectric breakdown. (B) SEM micrographs taken by milling the trench to: (1) 30 μm from the pinhole: small voids are found. (2) 14 μm: approaching the pinhole voids are larger and are mostly parallel to layers. (3) 7.5 μm: larger voids are accompanied by extensive layer delamination and additional delamination of neighboring layers. [Color figure can be viewed in the online issue, which is available at wileyonlinelibrary.com.]

The features observed in the wall of the pinhole in Figure 5 were examined in more detail. To spatially resolve the changes in the polymer structure as a function of distance from the breakdown site, FIB was used to mill a trench with a face about 50 μm from the pinhole. An SEM image was recorded of the face, and then the trench was extended in a stepwise manner toward the breakdown pinhole by serial ion milling. The procedure is illustrated in Figure 6A. A total of 38 sequential SEM images were recorded between the milling steps. The images were separated by between 500 nm and 2000 nm, with closer steps when the features were evolving rapidly. The first image, 50 μm from the breakdown site, showed a layer structure like that seen in the control films. The first evidence for breakdown-induced changes was found about 30–35 μm from the breakdown (Fig. 6B1). This consists of isolated small voids within the layers. At about 14 μm (Fig. 6B2), a larger void is apparent along a layer interface. The layer structure adjacent to the void remains intact, but it is deformed to accommodate the delaminations. The sequence of images showed that this feature was near the end of a continuous channel that emanated from the pinhole. The size of the void as well as the extent of the deformations of nearby layers varies with the distance from the pinhole. Figure 6B3 illustrates this channel closer to the pinhole.

In the image in Figure 6B3 of this channel at 7.5 μm from pinhole, the void and the layer deformations are larger. In addition, a second void is seen adjacent to the first. These two voids appear to be associated. Figure 7 shows an enlargement of this cross section where the individual layers have been highlighted to make it easier to follow the interfaces. There is an intact P[VDF-HFP] layer between the two voids. The second delamination forms at an interface adjacent to the initial one such that this single layer, in this case P[VDF-HFP], forms the top layer of one void and the bottom layer of another.

The existence of delaminations in adjacent layers appears to be analogous to "cooperative delamination" processes that have been observed in studies of the mechanical properties of layered polymers. Similar cooperative layer delaminations have been observed in studies of the effects of mechanical stress on both PC/polymethylmethacrylate (PMMA) and PC/styrene-co-acrylonitrile (SAN) multilayer films.[25] The analogy to mechanical processes is not surprising; the propagation of the voids out from the pinholes and even the large electric fields themselves will create substantial mechanical stress within the films. The effect of layering on the mechanical properties may play an important role in determining the breakdown pathways and ultimately the dielectric strength of the multilayer composites.

The images of the pinhole after a breakdown (Fig. 5) showed voids extending through the pinhole walls. Figure 8 shows a quasi-3D picture of the features near a pinhole to illustrate the typical features, and how they propagate into the film. This figure was constructed from a set of 30 images starting at a breakdown pinhole and extending 16.15 μm back

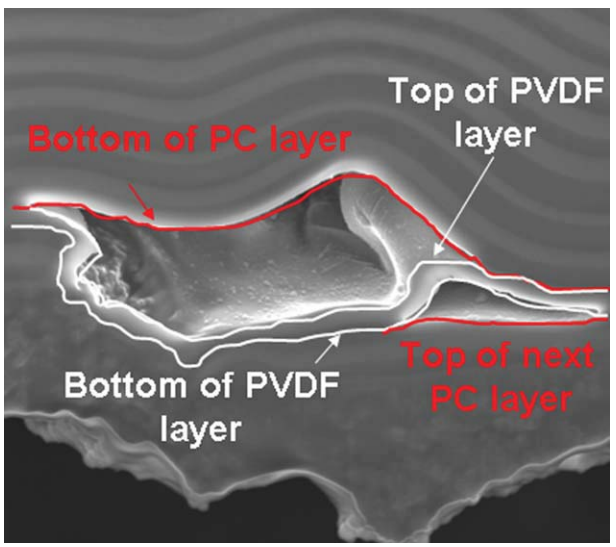

Figure 7 SEM micrograph illustrating a cooperative layer delamination of the void shown in Figure 6B, located about 7.5 μm from pinhole. [Color figure can be viewed in the online issue, which is available at wileyonlinelibrary.com.]

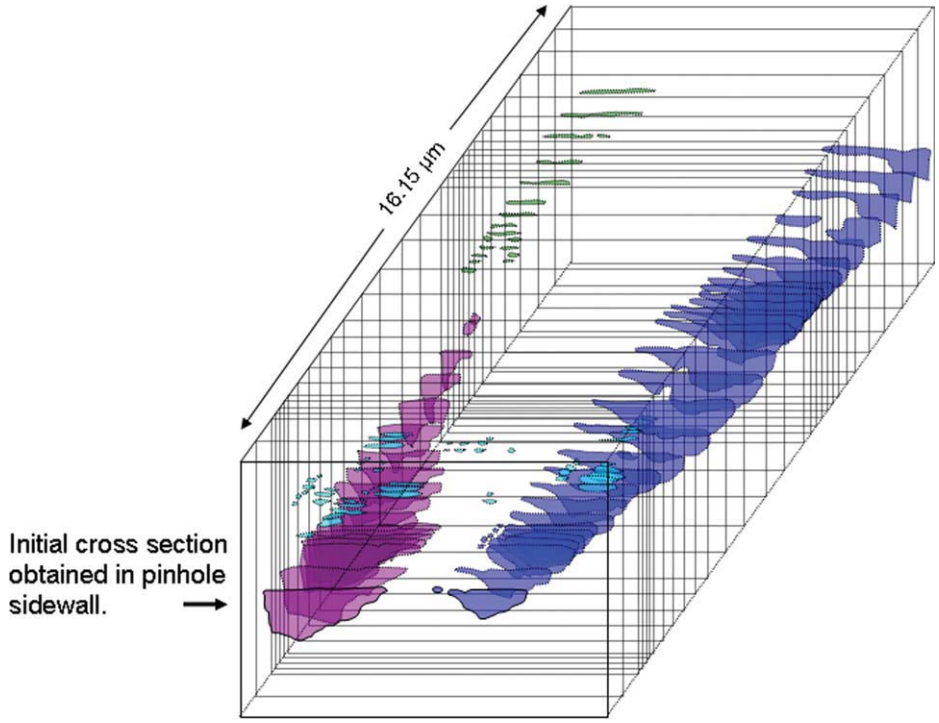

Figure 8 A reconstruction of voids and layer delaminations as a function of distance from a breakdown pinhole with the closest cross section milled directly in the pinhole sidewall. The reconstruction features 30 successive FIB milling cross sections covering a distance of 16.15 μm in length.

into the film. The breakdown site in this case is from a different sample than the one shown in Figure 5; it was selected to show the propagation of the principal features clearly. To show how the voids propagate through the film, they were outlined in color, and the remainder of the cross section (which displayed still layered polymer) is suppressed. This gives a quasi-3D reconstruction illustrating how the location, size, and shape of the voids vary as they extend out into the sample. The voids are seen to extend laterally, parallel to the film surface, and back into the film.

Two of the channels shown in Figure 8, in maroon and dark blue, are connected into the pinhole. These voids diverge from the main discharge path across the film (at the pinhole). In the region within a few μm of the breakdown pinhole such voids are numerous and some extend more than ~ 15 μm away from the breakdown site. Outside of the pinhole, the breakdown-induced voids run laterally, approximately parallel to layers, in a direction that was perpendicular to the electric field gradient. Virtually all of the larger features are found at or near the interfaces between layers and are formed by layer delaminations.

In addition to features that form a continuous channel from the breakdown pinhole, Figure 8 also shows self-contained channels that do not start within the pinhole. These isolated features increase and then decrease in size within the film. These isolated voids were also along layer boundaries and were associated with layer delaminations. Some of the localized voids extend for a few micrometers. Others, for example those imaged in Fig. 8 in light blue, remain as small voids with diameters on the order of 500 nm. The self-contained voids that do not emanate from the pinhole probably arise from prebreakdown discharges that occur at random within the film, but whose propagation was interrupted when the main breakdown occurred.

It is of some interest that none of the voids that were imaged appeared to be associated with the type of defects that were found in images of the pristine films (Fig. 3). Although a contribution to a breakdown from such defects cannot be ruled out, the concentration of localized voids was much higher than the density of defects in the pristine films.

A smaller set of FIB/SEM images were obtained from samples where the breakdown occurred with the PC surface in contact with the positively charged tip. In this orientation, the surface of the film shows tree-like damage features extending out from the pinhole. Example SEM micrographs of a 32-layer 50 vol % PC/50 vol % P[VDF-HFP] film after a breakdown with a PC layer near a positive tip are shown

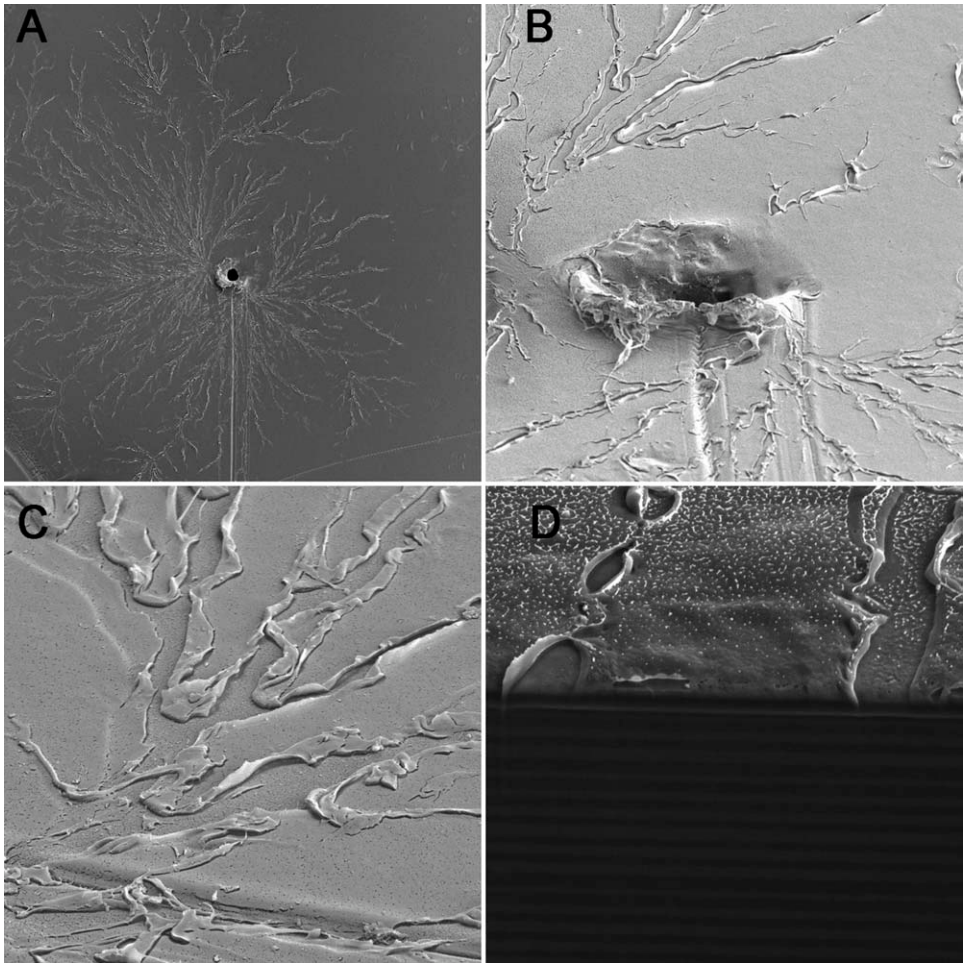

Figure 9 SEM micrographs of a 32-layer 50 vol % PC/50 vol % P[VDF-HFP] film after a breakdown with a PC layer near a positive tip. (A) Breakdown pinhole showing surface damage (treeing). (B) Breakdown pinhole and treeing. (C) Close-up of treeing showing the top-most PC layer blown away and folded onto itself. (D) FIB-prepared cross section $\sim$ 40 μm from the pinhole. Here, the damage is localized to the interface between the topmost PC layer and the first underlying P[VDF-HFP] layer. (A) was obtained with the e-beam normal to the surface, for the others the e-beam was at 52° with respect to the surface.

in Figure 9. The SEM images of the surface in Figure 9A are consistent with the optical microscopic images shown in Reference [3].

In the images in Figure 9B and C, the majority of the damage is localized near the surface. In fact, the topmost PC layer is mostly removed in channels that radiate outward from the pinhole. Figure 9C is a close-up near the pinhole showing that the topmost PC layer in the channels has blown away and folded onto itself. Presumably, this damage results from a charge propagating outward from the pinhole along the interface between the topmost PC and underlying P[VDF-HFP] layer. The sample shows extensive surface damage, and the FIB/SEM image (Fig. 9D) shows that below the surface, the internal layer structure is largely intact in areas neighboring the breakdown pinhole and beyond.

Comparing Figure 9 with the earlier images shows that when the PC layer is next to the positive pin electrode, the observed damage appears to be qualitatively different from that when the P[VDF-HFP] is next to the pin. In either case, the damage propagates along interfaces; the difference is that with the PC layer nearest the high-voltage needle, the breakdown is diverted at the first interface, whereas with the P[VDF-HFP] layer at the surface, the breakdown penetrates farther into the film and is diverted at multiple interfaces. The differences due to the polarity of the applied field seem likely to be due to electrical effects, perhaps differences in the barrier to charge injection between PC and P[VDF-HFP] or in the relative charge transport efficiency along and across the interfaces. Because the inhomogeneity of the breakdown field may also contribute, it is of interest to examine the damage due to a breakdown using a more homogeneous field.

DISCUSSION

In the classical picture of dielectric breakdown in a polymer,[24] when the applied field approaches

breakdown, small discharges occur at random within the polymer material. The voids they produce serve as the origin of prebreakdown processes where further partial discharges progress through the dielectric, opening up a void with a path whose form resembles a tree. When this tree bridges the film, dielectric breakdown, a large discharge, can occur along this conducting path across the film. The dielectric breakdown results in the 30–70 μm pinhole observed in these films.

The FIB/SEM technique allows us to image details of the damage caused by a breakdown in these polymer materials. In the homogeneous materials, the breakdown path more or less follows the field gradient directly across the film such that the tree was within the breakdown pinhole and evidence for it does not survive the breakdown. In the multilayer polymers, the breakdown-induced damage is found extending through the pinhole walls and extending well away from the breakdown site. The damage runs mostly along layer interfaces. The location of this extended damage depends on the orientation of the polymer film in the inhomogeneous field. With the P[VDF-HFP] film in contact with the high-voltage tip, the damage outside the pinhole is found distributed internally, across the thickness of the film. With the PC layer contacting the high-voltage pin, the extended damage is found primarily at the surface and first interface. In both cases, the images suggest that the interface boundaries provide a path for the breakdown processes.

The images show that the multilayer structure can significantly alter the dielectric breakdown processes in the film. The layer boundaries appear to provide a path that can deflect a breakdown to propagate laterally in the film. This is consistent with a mechanism for the increased dielectric strength via the classical "barrier effect." The barrier effect has been studied extensively and was recently reviewed.[6,26] An increase in the dielectric strength of a material can be achieved by the introduction of an additional insulation (a barrier) placed within the bulk of the material. Although the details of the mechanism depend on the materials involved, it is generally accepted that a barrier is effective, because it impedes the propagation of the electrical breakdown channel across the material.

The small self-contained voids that appeared within the film but do not connect with the breakdown pinhole are possibly prebreakdown events. Because the dielectric strength of the multilayer polymer is larger than that of either of the component polymers, it is reasonable to find evidence for more than one initiation point. Smaller channels that are not connected directly to the breakdown pinhole apparently did not have time to propagate and initiate the breakdown event.

CONCLUSIONS

We have demonstrated that FIB milling in conjunction with SEM imaging is a useful technique to image layer structure and the effects of a dielectric breakdown in multilayer polymer PC/P[VDF-HFP] dielectric materials. Sequential cross sections allow for tracing nano- to micrometer sized features across microscopic distances in films subjected to a breakdown. FIB/SEM also permitted an assessment of defects within pristine layered films before they were subjected to an electric field. The defects in pristine films were rare instances of inclusions at concentrations of $\sim$ 0.01% in the P[VDF-HFP] layers and at a few ppm in the PC layers. No defects associated with the interfacial regions or involving delaminations or layer discontinuities were found.

FIB/SEM images of homogeneous and multilayer films make clear some significant differences in the effects of a breakdown on the multilayered films. The damage due to a breakdown in homogeneous films was confined to the pinhole site; no features extending beyond the pinhole walls were observed. Sequential SEM images of a 32-layer 50/50 PC/P[VDF-HFP] film after a breakdown when the positive charge was in contact with the P[VDF-HFP] showed voids through the pinhole walls that extended laterally $\sim$ 15 μm or more away from the breakdown site. The images provide evidence that the layer interfaces alter the path of a dielectric breakdown in the multilayer films. They appear to deflect the propagation of the breakdown directly across the film. This is consistent with a barrier effect contributing to the dielectric strength.

The voids were primarily along layer interfaces and involved considerable layer delamination. The presence of layer delamination suggests that the mechanical properties of the interfaces may play a role in the effectiveness of the barriers. There was also evidence for cooperative delamination processes, previously observed in studies of mechanical deformations of multilayer films. Otherwise, near the delaminations, the layer structure remains, but is distorted to accommodate the voids. The dependence of the observed damage on the polarity and film orientation of the multilayer film, both here and in the previous article confirm that the electrical properties of the multilayers play a role in the effectiveness of the barriers.

In materials that include a barrier effect, the dielectric strength will depend on the effectiveness of the barriers. In general, factors such as the barrier composition, positions, layer thicknesses, permittivities, and conductivities of the barrier material will influence its effectiveness. The FIB/SEM images suggest that it is the layer interfaces that play a key role in acting as the barriers in PC/P[VDF-HFP] films.

Thus, modifying the mechanical and electrical properties of the interfaces may be a useful strategy to further improve the dielectric properties of these dielectric materials.

We thank the Office of Naval Research for support of this work. Case-Western Reserve University also acknowledges the support of the National Science Foundation.

References

1. Jain, P.; Rymaszewski, E. J. Thin Film Capacitors for Packaged Electronics; Kluwer Academic Publishers: Norwell, MA, 2003.
2. Wolak, M. A.; Pan, M. -J.; Wan, A.; Shirk, J. S.; Mackey, M.; Hiltner, A.; Baer, E.; Flandin, L. Appl Phys Lett 2008, 92, 113301.
3. Mackey, M.; Hiltner, A.; Baer, E.; Flandin, L.; Wolak, M. A.,Shirk, J. S. J Phys D: Appl Phys 2009, 42, 175304.
4. Vogelsang, R.; Farr, T.; Frohlich, K. IEEE Trans Dielectr Electr Insul 2006, 13, 373.
5. Flandin, L.; Vouyovitch, L.; Beroual, A.; Bessede, J. L.; Alberolal, N. D. J Phys D: Appl Phys 2005, 38, 144.
6. Lebedev, S. M.; Gefle, O. S.; Pokholkov, Y. P. IEEE Trans Dielectr Electr Insul 2005, 12, 537.
7. Gefle, O. S.; Lebedev, S. M.; Pokholkov, Y. P.; Gockenbach, E.; Borsi, H. J Phys D: Appl Phys 2004, 37, 2318.
8. Agoris, D. P.; Vitellas, I.; Gefle, O. S.; Lebedev, S. M.; Pokholkov, Y. P. J Phys D: Appl Phys 2001, 34, 3485.
9. Yeoh, T. S.; Chaney, J. A.; Leung, M. S.; Ives, N. A.; Feinberg, Z. D.; Ho, J. G.; Wen, J. J Appl Phys 2007, 102, 123104.
10. Giannuzzi, L. A.; Prenizter, B. I.; Kempshall, B. W. Introduction to Focused Ion Beams: Instrumentation, Theory, Techniques and Practice; Springer: New York,2005.
11. Aubry, C.; Trigaud, T.; Moliton, J. P.; Chiron, D. Syn Met 2002, 127, 307.
12. Pialat, E.; Trigaud, T.; Bernical, V.; Moliton, J. P. Mater Sci Eng C 2005, 25, 618.
13. Pialat, E.; Trigaud, T.; Moliton, J. P.; Thevenot, M. J Polymer Sci B: Polymer Phys 2007, 45, 2993.
14. Brostow, W.; Gorman, B. P.; Olea-Mejia, O. Mater Lett 2007, 61, 1333.
15. Brunner, S.; Gasser, P.; Simmler, H.; Wakili, K. B. Surf Coat Technol 2006, 200, 5908.
16. Liu, R. Y. F.; Jin, Y.; Hiltner, A.; Baer, E. Macromol Rapid Commun 2003, 24, 943.
17. Liu, R. Y. F.; Ranade, A. P.; Wang, H. P.; Bernal-Lara, T. E.; Hiltner, A.; Baer, E. Macromolecules 2005, 38, 10721.
18. Jesse, S.; Guillorn, M. A.; Ivanov, I. N.; Puretzky, A. A.; Howe, J. Y.; Britt, P. F.; Geohegan, D. B. Appl Phys Lett 2006, 89, 013114.
19. Seiler, H. J Appl Phys 1983, 54, R1.
20. This effect is similar to charge contrast imaging, which has been used to distinguish single walled carbon nanotubes from polystyrene in blends. See: Loos, J.; Alexeev, A.; Grossiord, N.; Koning, C. E.; Regev, O. Ultramicroscopy 2005, 2, 160.
21. Zumbrunnen, D. A.; Inamdar, S. Chem Eng Sci 2001, 56, 3893.
22. Topographical contrast in SEM is due to differences in the collection efficiency of secondary electrons based on the relative proximity of the sample to the detector. In the case of the polypropylene (PP)/ethylene-propylene-diene-terpolymer (EPDM) multilayer described in Ref. 21, cryogenic fracture of the film yielded a cross-section where the individual PP and EPDM layers had distinct textures due to their differing fracture mechanics.
23. White, J.; Thomas, E. Rubber Chem Tech 1984, 57, 457.
24. Dissado, L. A.; Fothergill, J. C. Electrical Degradation and Breakdown in Polymers; Redwood Press: London, 1992.
25. Kerns, J.; Hsieh, A.; Hiltner, A.; Baer, E. J Appl Polymer Sci 2000, 77, 1545.
26. Vogelsang, R.; Farr, T.; Frohlich, K. IEEE Trans Dielectr Electr Insul 2006, 13, 373.